acid–base system may be used to explore the dependence of the acid–base character on composition. However, in the considered sodium phosphate melts this approach is impractical due to the high volatility of P_2O_5 at 800–850° and the chemically aggressive character of Na_2O. Instead we have made use of the strong acid WO_3 as a basicity probe.

When small amounts of solid WO_3 are added to the phosphate melt, acid–base reactions may occur according to a scheme of the type

phosphate-I (in melt) + WO_3(s) = phosphate-II (in melt) + WO_4^{2-} (in melt)

If WO_3 is a stronger acid than phosphate-II, this reaction will proceed to the right and might be expected to be associated with a certain evolution of heat. On the other hand, if phosphate-II is a stronger acid than WO_3, the reaction would have a tendency to proceed in the opposite direction. In this way the sign and magnitude of the enthalpy of solution of WO_3 may be used to survey the acid–base properties of the melt.

Let us now return to Figure 3, which gives the enthalpy of solution of solid WO_3 in sodium metaphosphate–pyrophosphate melts with mole fractions of Na_2O ranging from 0.50 to 0.61. At $N_{Na_2O} = 0.50$ the enthalpy of solution is +3.8 kcal/mol. This reflects the fact that P_2O_5, the corresponding acid to PO_3^-, is a very strong acid. As the mole fraction of Na_2O increases above 0.50, there is a sharp drop in the enthalpy of solution to −0.6 kcal at $N_{Na_2O} = 0.51$ and to −1.6 kcal at $N_{Na_2O} = 0.52$. Clearly the melt now contains significant amounts of a higher phosphate (presumably $P_2O_7^{4-}$), which will react with the added WO_3 to yield the weaker acid PO_3^- and WO_4^{2-}. From about $N_{Na_2O} = 0.56$ to $N_{Na_2O} = 0.61$ the enthalpy of solution of WO_3 is essentially independent of composition, which reflects that the melt now contains two phosphate anions in comparable amounts, *i.e.*, it has buffer properties. At 843° the liquid range of the phosphate melts extends only to about $N_{Na_2O} = 0.63$. Therefore we were unable to explore at this temperature the interesting composition range near $N_{Na_2O} = 0.67$ associated with very high concentrations of pyrophosphate.

Acknowledgments.—We are indebted to Miss M. C. Bachelder, who carried out the chemical analyses, and to Mr. James Loehlin, who gave us valuable assistance in the evaluation of the X-ray structural data. This work has been supported by the National Science Foundation, the Army Research Office, Durham, N. C., and the Petroleum Research Fund, administered by the American Chemical Society. It also has benefited from the general support of Materials Science at The University of Chicago provided by the Advanced Research Projects Agency, Department of Defense.

CONTRIBUTION FROM THE DEPARTMENT OF CHEMISTRY, CORNELL UNIVERSITY, ITHACA, NEW YORK 14850

Matrix Isolation Study of Borazine and Boroxine. A Vibrational Analysis

BY ANDREW KALDOR* AND RICHARD F. PORTER

Received July 13, 1970

A vibrational analysis of borazine based on the infrared spectra of matrix-isolated isotopic species $H_3B_3N_3H_3$, $H_3{}^{10}B_3N_3H_3$, and $D_3B_3N_3H_3$ and the gaseous Raman spectrum of $H_3B_3N_3H_3$ is presented. One of the E′ modes, ν_{16}, is reassigned to 1068 cm^{-1}. Two of the inactive A_2' modes, ν_8 and ν_7, are assigned to 1195 and 782 cm^{-1}, respectively. The literature assignment of the other modes is confirmed, although the position of the A_1' and E″ modes is slightly modified. Strong bands observed in the matrix spectrum of borazine in the regions 1440 and 2500 cm^{-1} but not resolved in the gas-phase spectra are satisfactorily interpreted as combination bands for a planar D_{3h} molecule without invoking matrix effects or postulating a species of lower symmetry. By using the information available for borazine it is possible, through a combination-band analysis, to assign all the fundamentals of boroxine.

Introduction

The gas-phase infrared and liquid Raman spectra of borazine, $H_3B_3N_3H_3$, were first investigated by Crawford and Edsall.[1] The molecule was assumed to be isoelectronic with benzene, with point group D_{3h}. The symmetric planar structure was proposed by Bauer on the basis of early electron diffraction studies.[2] The infrared spectra were reinvestigated by Price and coworkers,[3] as well as by Silberman.[4] These studies essentially confirmed the Crawford–Edsall assignments. Kartha, *et al.*, on the basis of observed band shapes and isotope effects reassigned absorption bands at 918, 713,

* Address correspondence to this author at National Bureau of Standards, Washington, D. C. 20234

(1) B. L. Crawford and J. T. Edsall, *J. Chem. Phys.*, **7**, 223 (1939).

(2) S. H. Bauer, *J. Amer. Chem. Soc.*, **60**, 524 (1938).

(3) N. C. Price, R. D. B. Fraser, T. S. Robinson, and H. C. Longuet-Higgins, *Discuss. Faraday Soc.*, **9**, 131 (1950).

(4) E. Silberman, *Spectrochim. Acta, Part A*, **23**, 2021 (1967).

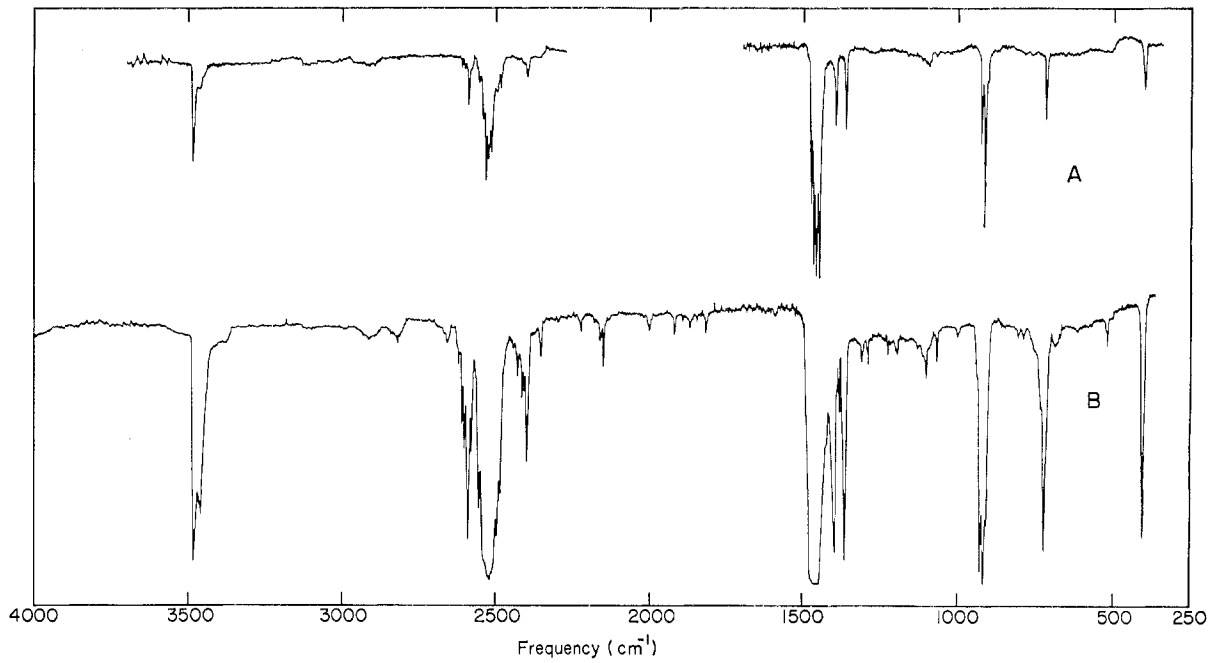

Figure 1.—Infrared spectra of borazine in argon matrix (M/R) = 1000) near 5°K after (A) 3-min deposition and (B) 30-min deposition.

and 393 cm^{-1} to A_2'' modes.[5] This left two E′ vibrational modes unassigned. Niedenzu and coworkers reported on extensive gas-phase infrared and liquid Raman spectroscopic studies of various isotopically labeled forms of borazine.[6] They have confirmed the assignments of Kartha, *et al.*, and have assigned all the active fundamentals. Recently Harshbarger, *et al.*,[7] have repeated the electron diffraction studies on borazine with improved techniques and the results cast doubt on the planar D_{3h} model. Their data indicate that the molecule has either C_2 symmetry, or it is planar with a large out-of-plane vibrational displacement. Another possible explanation is the presence of more than one isomeric form.

Electron diffraction studies on boroxine, $H_3B_3O_3$, which is isoelectronic with borazine, indicate this molecule to be planar with D_{3h} symmetry.[8] The gas-phase infrared spectrum of boroxine has been analyzed by Grimm, Barton, and Porter,[9] but no Raman spectrum of this unstable molecule has been obtained. Six of the seven infrared-active vibrational modes of boroxine have been assigned; one A_2'' has not been found.

In this paper a vibrational analysis of borazine based on matrix-isolation infrared spectra and gas-phase Raman data is presented. The matrix-isolation infrared spectrum of boroxine has also been obtained and is used for comparison with the borazine results. The anticipated advantages of the matrix-isolation technique are (a) better resolution of vibrational structure, (b) removal of hot bands, and (c) the observation of matrix effects on the symmetry of trapped molecules.

(5) V. B. Kartha, S. L. N. G. Krishnamachari, and C. R. Subramaniam, *J. Mol. Spectrosc.*, **23**, 149 (1967).

(6) K. Niedenzu, W. Sawodny, H. Watanabe, J. Dawson, T. Totani, and W. Weber, *Inorg. Chem.*, **6**, 1453 (1967).

(7) W. Harshbarger, G. Lee, R. F. Porter, and S. H. Bauer, *ibid.*, **8**, 1683 (1969).

(8) C. H. Chang, R. F. Porter, and S. H. Bauer, *ibid.*, **8**, 1689 (1969).

(9) F. A. Grimm, L. Barton, and R. F. Porter, *ibid.*, **7**, 1309 (1968).

Experimental Section

The experimental apparatus and procedures used in the matrix isolation experiments have been described elsewhere.[10] The matrix gases argon, xenon, and 20% argon–80% xenon were premixed with borazine in the M/R ratios 200/1, 500/1, 1000/1 and allowed to stand for 24 hr to ensure thorough mixing. The mixtures were then deposited on a CsI target window maintained near 5°K at the rate of 5–20 mmol/hr. Borazine was prepared by treating *B*-trichloroborazine with $NaBH_4$.[11] Samples of 96% enriched $H_3{}^{10}B_3N_3H_3$ and $D_3{}^{n}B_3N_3H_3$ (where n signifies natural abundance) were also prepared. The argon and xenon were obtained from the Matheson Co. Since boroxine is unstable at ordinary temperatures, it was prepared immediately prior to each experiment by the procedure of Barton, *et al.*,[12] by applying an electrical discharge to a low-pressure mixture of diborane and oxygen. Immediately after the explosion, argon was admitted into the sample bulb to the ratio of M/R = 1000. Spectra of $H_3B_3O_3$, $H_3{}^{10}B_3O_3$, and $D_3B_3O_3$ were obtained.

Infrared spectra were taken on a Perkin-Elmer 521 spectrophotometer, which was calibrated with CO, CO_2, and NH_3, as well as B_2H_6 impurity in the boroxine. The estimated uncertainty in measured frequencies is ±1 cm^{-1}. The Raman spectra were obtained on a Spex-Ramalog instrument.[13] The 488-nm argon line of a CRL 52MG laser was used as the excitation source. The laser beam was multipassed through the sample. The borazine sample was sealed at the saturation vapor pressure (200 mm) into a 5-cm long Pyrex cell with 2.4-cm diameter windows at each end.

Results

Weak and strong spectra of borazine in an argon matrix (M/R = 1000) near 5°K are shown in Figure 1. The observed frequencies of $H_3{}^{n}B_3N_3H_3$, $H_3{}^{10}B_3N_3H_3$, and $D_3B_3N_3H_3$ are listed in Tables I and II. Previously unreported structure near 1450 and 2500 cm^{-1} is evident. The 1450-cm^{-1} region at high resolution is

(10) A. Kaldor, I. Pines, and R. F. Porter, *ibid.*, **8**, 1418 (1969).

(11) G. H. Dahl and R. Schaeffer, *J. Inorg. Nucl. Chem.*, **12**, 380 (1960).

(12) L. Barton, F. A. Grimm, and R. F. Porter, *Inorg. Chem.*, **5**, 2076 (1966).

(13) The authors wish to express their appreciation to Dr. J. Allkins of Spex Industries, Inc., for his invaluable assistance in obtaining the gaseous Raman spectrum of borazine.

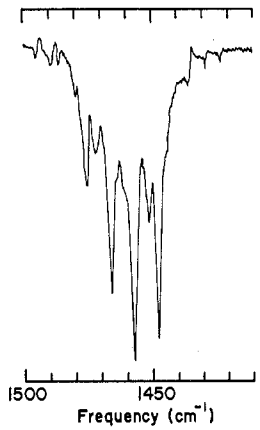

Figure 2.—High-resolution infrared spectrum of $H_3B_3N_3H_3$/Ar = 1/1000 near 5°K from 1400 to 1500 cm^{-1}.

shown in Figure 2. Due to the natural abundance of ^{10}B (20%) and ^{11}B (80%), four isotopic species are expected in the ratio $^{11}B_3:^{11}B_2{}^{10}B:^{11}B^{10}B_2:^{10}B_3$ = 64:48:12:1. The bands due to the mixed isotopic species are largely eliminated in the spectrum of 96% ^{10}B-enriched sample, shown in Figure 3 together with the gas-phase fundamentals. The effect of the matrix on the observed structures has been examined by varying the M/R ratio from 200 to 1000 and by using xenon in place of argon and mixed matrices of argon–xenon. The bands do not shift position, and the structures observed are essentially retained.

The spectra of normal boroxine and 96% ^{10}B-enriched boroxine in an argon matrix (M/R = 1000) near 5°K are shown in Figure 4. Structure similar to that

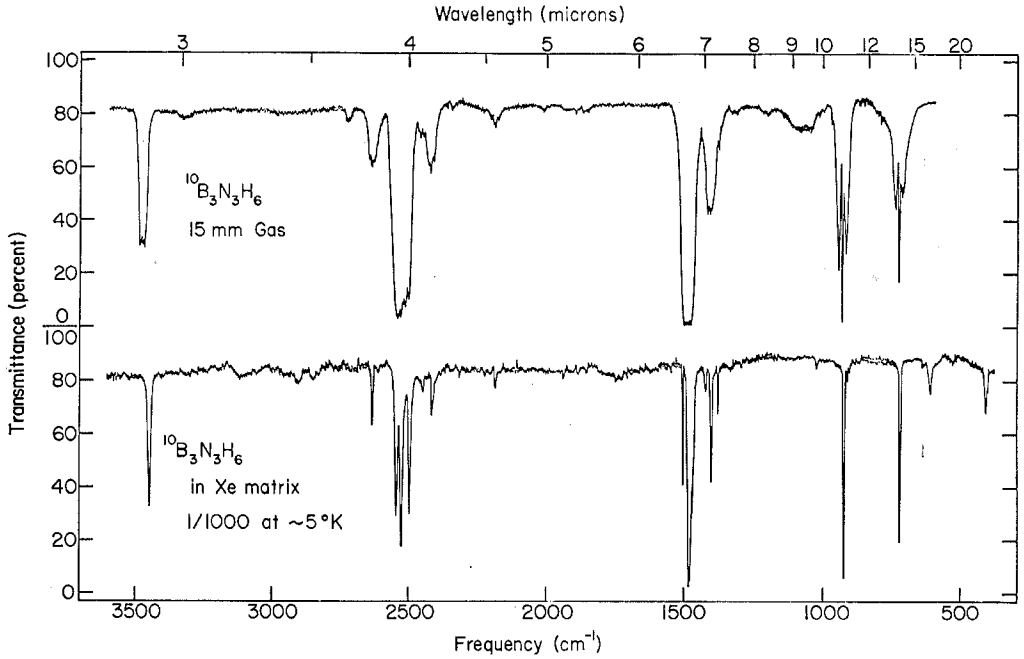

Figure 3.—Infrared spectra of $H_3{}^{10}B_3N_3H_3$.

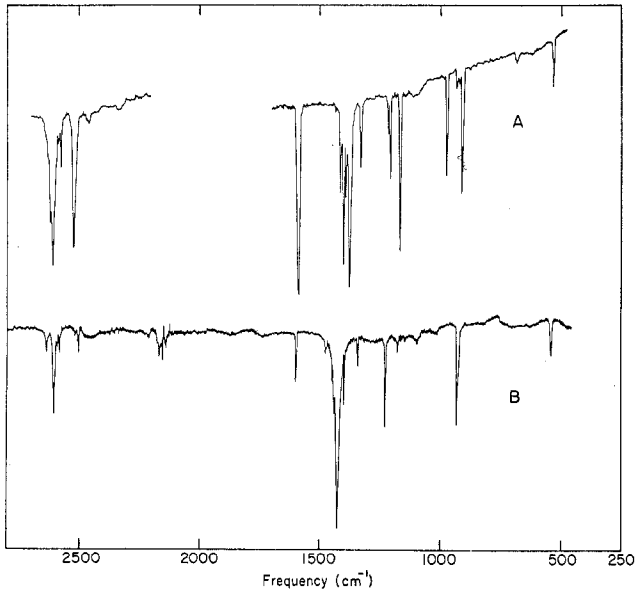

Figure 4.—Infrared spectra of (A) $H_3B_3O_3$/Ar = 1/1000 and (B) $H_3{}^{10}B_3O_3$/Ar = 1/1000 near 5°K.

found in borazine is also observed near 1400 and 2600 cm^{-1}. The observed frequencies of $H_3B_3O_3$ and $H_3{}^{10}B_3O_3$, along with the gas-phase fundamentals, are listed in Table III. Spectra for $D_3B_3O_3$ are given in Table IV.

With the exception of the spectral regions near 1400 and 2500 cm^{-1} the remainders of the infrared spectra of both borazine and boroxine are simple and similar to the gas-phase spectra. The 1450-cm^{-1} region in borazine and the 1380-cm^{-1} region in boroxine are associated with in-plane degenerate ring motions, and the 2500-cm^{-1} region in borazine and the 2600-cm^{-1} region in boroxine are associated with the degenerate B–H stretching modes. The other degenerate fundamentals do not exhibit this complex structure.

The observed gas-phase Raman spectrum for normal borazine is shown in Figure 5. The observed frequencies, along with the published liquid Raman lines, are listed in Table V.

Vibrational Assignments. Borazine.—Borazine, with D_{3h} symmetry, should have ten infrared active funda-

TABLE I
THE INFRARED SPECTRA OF $H_3B_3N_3H_3$ AND $H_3{}^{10}B_3N_3H_3$

$H_3{}^nB_3N_3H_3$ in Ar matrix	Assignment	$H_3{}^nB_3N_3H_3$ gas[a]	$H_3{}^{10}B_3N_3H_3$ gas[a]	Assignment	$H_3{}^{10}B_3N_3H_3$ in Ar matrix
403 s	$\nu_{16}(A_2'')$	394			
			396	$\nu_{10}(A_2'')$	406 m
518 w	$\nu_{17}(E')$	518			
525 vw, sh	$^{11}B_2{}^{10}B$				
			528	$\nu_{17}(E')$	528 w
683 vw, br	$\nu_{10} + \nu_{20}$ 403 + 280 = 683				
713 m	$^{11}B_2{}^{10}B$ resonance				
718 s	$\nu_9(A_2'')$	719			
721 sh	$^{11}B^{11}B$				
			725	$\nu_9(A_2'')$	724 vs
733 m, sh	$^{10}B_3$ + resonance				
788 vw	$\nu_{17} + \nu_{20}$ 518 + 280 = 798				
805 vw					
				$\nu_{17} + \nu_{20}$ 528 + 285 = 813	813 vw
905 s, sh	$^{11}B_2{}^{10}B$ resonance			$^{11}B_2{}^{10}B$	904 sh
913 vs	$\nu_8(A_2'')$	918		$^{11}B^{10}B_2$	910 sh
924 vs	$^{10}B_3$ + $^{11}B^{10}B_2$ resonance		930	$\nu_8(A_2'')$	926 vs
1000 vw, br	$\nu_{20} + \nu_9$ 280 + 718 = 998			$\nu_9 + \nu_{20}$ 724 + 285 = 1009	1009 vw
1068 w	$\nu_{18}(E')$			$\nu_{18}(E')$	1072 w
1102 m, br	$\nu_{15}(E')$	1096			
				$\nu_{15}(E')$	1106 w
1130 vw					
1192 w, br	$\nu_8 + \nu_{20}$ 913 + 280 = 1193				
				$\nu_8 + \nu_{20}$ 926 + 285 = 1211	1208 vw
1225 w	$\nu_4 + \nu_{10}$ 845 + 403 = 1248				
1289 w	$\nu_{17} + \nu_{13}$ 518 + 770 = 1288				
1294 sh	$^{11}B_2{}^{10}B$				
				$\nu_{17} + \nu_{14}$ 528 + 770 = 1298	1295 w
1310 w	$\nu_7 + \nu_{17}$ 782 + 518 = 1310				
				$\nu_7 + \nu_{17}$ 794 + 528 = 1322	1322 w
1363 m	$\nu_4 + \nu_{17}$ 845 + 518 = 1363				
1366 sh	$^{11}B_2{}^{10}B$				
1370 sh	$^{11}B^{10}B_2$				
1376 w, sh	$^{10}B_3$			$\nu_4 + \nu_{17}$ 848 + 528 = 1376	1376 m
1380 w	$\nu_{10} + \nu_{18}$ 403 + 977 = 1380 or $\nu_{20} + \nu_{15}$ 280 + 1102 = 1382				
1387 sh	$^{11}B_2{}^{10}B$				
				$\nu_{10} + \nu_{18}$ 406 + 985 = 1391 or $\nu_{15} + \nu_{20}$ 1106 + 285 = 1391	1391 m
1396 s, sh	$^{11}B_2{}^{10}B$ resonance				
1398 s	$\nu_{14}(E')$	1406			
1402 sh	$^{11}B^{10}B_2$				
			1408	$\nu_{14}(E')$	1404 s, 1420 w
1448 vs	$\nu_3 + \nu_{17}$ 940 + 518 = 1458				
1452 s, sh	$^{11}B_2{}^{10}B$				
1458 vs	$\nu_{13}(E')$	1465		$^{11}B_3$	1458 vw, sh
1461 sh					1461 w, sh

TABLE I (*Continued*)

$H_3{}^nB_3N_3H_3$ in Ar matrix	Assignment	$H_3{}^nB_3N_3H_3$ gas[a]	$H_3{}^{10}B_3N_3H_3$ gas[a]	Assignment	$H_3{}^{10}B_3N_3H_3$ in Ar matrix
1466 s	$^{11}B_2{}^{10}B$			$^{11}B_2{}^{10}B$	1468 vw, sh
1472 m, sh					
1476 m	$^{11}B^{10}B_2$			$^{11}B^{10}B_2$	1476 s, sh
1480 vw, sh					1480 sh
1486 vw, sh	$^{10}B_3$		1488	$\nu_{13}(E')$	1486 vs
1490 w, br	$\nu_9 + \nu_{19}$ 718 + 770 = 1488				
1495 vw	$\nu_{17} + \nu_{18}$ 518 + 977 = 1495				
				$\nu_3 + \nu_{17}$ 974 + 528 = 1502	1502 s
				$\nu_{18} + \nu_{17}$ 985 + 528 = 1513	1520 vw
1590 vw	$\nu_{16} + \nu_{17}$ 1068 + 518 = 1586			$\nu_{16} + \nu_{17}$ 1072 + 528 = 1600	1599 vw
1818 w, br				$\nu_8 + \nu_{19}$ 926 + 770 = 1696	1696 vw
1848 vw	$\nu_3 + \nu_8$ 940 + 913 = 1853 or $\nu_7 + \nu_{16}$ 782 + 1068 = 1850			$\nu_9 + \nu_{18}$ 724 + 985 = 1709	1710 vw
1871 w, br	$\nu_{15} + \nu_{19}$ 1102 + 770 = 1872			$\nu_{18} + \nu_{19}$ 985 + 770 = 1755	1750 vw, br
1890 vw	$\nu_8 + \nu_{18}$ 913 + 977 = 1890			$\nu_{16} + \nu_{19}$ 1072 + 770 = 1842	1850 vw
1921 w	$\nu_4 + \nu_{16}$ 845 + 1068 = 1913 or $\nu_{14} + \nu_{17}$ 1394 + 518 = 1912			$\nu_7 + \nu_{16}$ 794 + 1072 = 1866	1864 vw
				$\nu_{14} + \nu_{17}$ 1404 + 528 = 1932	1932 vw
2002 w, br	$\nu_3 + \nu_{16}$ 940 + 1068 = 2008				
2146 m	$2\nu_{16}$ 2(1068) = 2136				
2158 w	$\nu_{14} + \nu_{19}$ 1394 + 770 = 2164				
2168 vw	$\nu_{15} + \nu_{16}$ 1102 + 1068 = 2170				
2175 vw	$\nu_7 + \nu_{14}$ 782 + 1394 = 2176			$\nu_7 + \nu_{14}$ 794 + 1404 = 2198	2194 w
2218 w	$\nu_{13} + \nu_{19}$ 1458 + 770 = 2228				
2230 vw	$\nu_{11} + \nu_{14}$ 845 + 1394 = 2239 or $^{11}B_2{}^{10}B$				2320 vw
2352 w				$\nu_8 + \nu_{14}$ 974 + 1404 = 2378	2370 vw, br
2398 s	$\nu_8 + \nu_{13}$ 940 + 1458 = 2398				
2408 m	$^{11}B_2{}^{10}B$				
2416 m	$^{11}B^{10}B_2$				
2421 vw, sh	$^{10}B_3$				2422 m
2430 w	$\nu_{13} + \nu_{18}$ 1458 + 977 = 2435				
2438 sh	$^{11}B_2{}^{10}B$				
2449 vw	$^{11}B^{10}B_2$				
				$\nu_8 + \nu_{13}$ 974 + 1486 = 2460	2452 w
2483 m	$\nu_{14} + \nu_{15}$ 1394 + 1102 = 2496				
2491 sh	$^{11}B_2{}^{10}B$				
2498 s, sh	$^{11}B^{10}B_2$				
				$\nu_{14} + \nu_{15}$ 1404 + 1106 = 2510	2501 vs
2513 vs	$\nu_{12}(E')$	2520			
2518 sh	$^{11}B_2{}^{10}B$				2518 vw
2522 vs, 2532 vs	$\nu_{13} + \nu_{16} + {}^{11}B^{10}B_2$ 1458 + 1068 = 2526		2535	$\nu_{12}(E')$	2529 vs

TABLE I (*Continued*)

$H_3{}^nB_3N_3H_3$ in Ar matrix	Assignment	$H_3{}^nB_3N_3H_3$ gas[a]	$H_3{}^{10}B_3N_3H_3$ gas[a]	Assignment	$H_3{}^{10}B_3N_3H_3$ in Ar matrix
2540 s, sh					
				$\nu_{13} + \nu_{16}$ 1486 + 1072 = 2558	2549 vs
2554 m, br	$\nu_{13} + \nu_{15}$ 1458 + 1102 = 2560				
2560 sh	$^{11}B_2{}^{10}B$				
2565 sh	$^{11}B^{10}B_2$				
2579 m	$^{11}B_2{}^{10}B$ resonance				
2589 s	$\nu_6 + \nu_{14}$ 1195 + 1394 = 2589			$\nu_{15} + \nu_{13}$ 1106 + 1486 = 2592	2590 vw
2602 m	$^{11}B_2{}^{10}B$ resonance				
2612 m, 2622 w, 2627 vw	Isotopic resonance				
				$\nu_6 + \nu_{14}$ 1237 + 1404 = 2641	2641 m
2660 w, br	$\nu_6 + \nu_{13}$ 1195 + 1458 = 2653				
2669 vw	$^{11}B_2{}^{10}B$			$\nu_6 + \nu_{13}$ 1237 + 1486 = 2723	2710 vw
2820 vw, br				$\nu_4 + \nu_{12}$ 848 + 2529 = 3377	3380 vw
3457 s, br	$\nu_3 + \nu_{12}$ 940 + 2513 = 3453				
3465 s, sh	$^{11}B_2{}^{10}B$				
3482 s	$\nu_{11}(E')$	3486	3486	$\nu_{11}(E')$	3482 s
				$\nu_3 + \nu_{12}$ 974 + 2529 = 3503	3503 sh

[a] Gas data from ref 6.

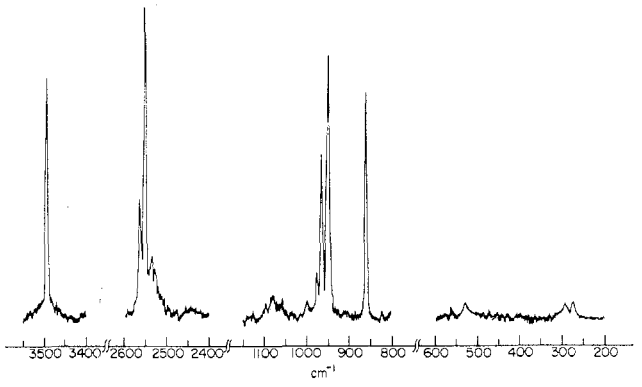

Figure 5.—Raman spectrum of gaseous borazine.

mentals (3 A_2'' + 7 E'), fourteen Raman-active ones (4 A_1' (p) + 7 E' (dp) + 3 E'' (dp)), and three which are inactive (3 A_2'). The assignment of the A_2'' vibrations is that of Kartha, *et al.*,[5] based on band shapes. These are observed as single bands at 403, 718, and 913 cm^{-1} in the matrix. Six of the seven E' vibrational species assigned by Niedenzu, *et al.*,[6] are confirmed. These are at 3482, 2513, 1458, 1394, 1102, and 518 cm^{-1} compared to the gas phase at 3486, 2520, 1465, 1406, 1096, and 518 cm^{-1}, respectively. Niedenzu, *et al.*, reported ν_{16} at 990 cm^{-1},[6] but in the matrix no corresponding band is observed. A very weak band at 1000 cm^{-1} can readily be assigned to $\nu_9 + \nu_{20}$. The weak band at 1068 cm^{-1} upon *B*-deuteration shows a large shift to 812 cm^{-1}. In the gas-phase Raman spectrum the 1068-cm^{-1} band is depolarized, and its band shape is similar to those of the other observed E' mode at 518 cm^{-1}. From the Raman spectrum the position of the A_1' modes in the gas phase was found shifted from the reported liquid frequencies. The symmetric N–H stretch, ν_1, and the B–H stretch, ν_2, were observed in the gas phase at 3488 and 2545 cm^{-1} compared with the observed frequencies in the liquid at 3453 and 2535 cm^{-1}, respectively. The ν_3 and ν_4 modes were observed, respectively, at 942 and 857 cm^{-1} in the gas phase, at 940 and 852 cm^{-1} in the liquid, and in combination at 940 and 845 cm^{-1} in the matrix. The E'' modes in the gas-phase Raman spectrum were observed at 987, 787, and 280 cm^{-1}. Niedenzu, *et al.*, have reported these fundamentals in the liquid at 968, 798, and 288 cm^{-1}. They have identified the 968-cm^{-1} band by polarization measurements since a disproportionately large fraction of that band remained, indicating a depolarized component.[6] Polarization measurements on the gas spectrum indicated the entire 968-cm^{-1} band as being polarized. In the matrix, in combination, the E'' modes, ν_{18}, ν_{19}, and ν_{20}, were found at 977, 770, and 280 cm^{-1} respectively.

Using combination bands it was possible to estimate the positions of two of the three inactive A_2' modes. These are ν_6 at 1195 cm^{-1} and ν_7 at 782 cm^{-1}.

The assigned frequencies of matrix-isolated borazine for the three isotopic species considered here are summarized in Table VI. The product rule was applied where possible and the results are tabulated in Table VII.

Boroxine.—Group theory predicts for boroxine seven infrared-active fundamentals (5 E' + 2 A_2'') and ten Raman-active ones (3 A_1' + 5 E' + 2 E''); two are expected to be inactive (2 A_2'). Grimm, *et al.*,[9] have been able to identify only one of the two expected A_2''

TABLE II

THE INFRARED SPECTRUM OF $D_3B_3N_3H_3$

$D_3B_3N_3H_3$ in Ar matrix	Assignment	$D_3B_3N_3H_3$ gas[a]	$D_3B_3N_3H_3$ in Ar matrix	Assignment	$D_3B_3N_3H$ gas[a]
330 m, br	$\nu_{10}(A_2'')$	327	1450 s, sh	$^{11}B_2{}^{10}B$	
507 w	$\nu_{17}(E')$	509	1457 sh	Partially deuterated species	
713 m	$\nu_9(A_2'')$	716			
716 sh	$^{11}B_2{}^{10}B$		1460 s, sh	$^{11}B^{10}B_2$	
719 sh	$^{11}B^{10}B_2$		1467 m, sh	$2\nu_{18}$, 2(734) = 1468	
724 sh	$^{10}B_3$				
767 vw	$\nu_{17} + \nu_{20}$ 507 + 260 = 767		1476 m, sh	$^{10}B_3$ + 713 + 760 = 1473	
			1548 w	$\nu_4 + \nu_9$ 845 + 713 = 1558	
779 w, sh 788 w, sh 793 vw, sh	Partially deuterated species		1840 w	$\nu_{14} + \nu_{17}$ 1326 + 507 = 1833	
803 vs	$\nu_8(A_2'')$	808	1876 w	$\nu_4 + \nu_{15}$ 845 + 1019 = 1864	
808 s, sh	$^{11}B_2{}^{10}B$				
812 s, sh	$\nu_{16}(E')$		1900 sh		
814 sh	$^{11}B^{10}B_2$		1905 sh		
913 m 925 w	Partially deuterated species		1912 vs	$\nu_{12}(E')$	1897
			1921 sh	$\nu_8 + \nu_{15}$ 904 + 1020 = 1924	
1020 w	$\nu_{15}(E')$	1022			
1275 w	$\nu_{15} + \nu_{20}$ 1020 + 260 = 1280		1932 s, sh	$^{11}B_2{}^{10}B$	
			1937 sh	$^{11}B^{10}B_2$	
1326 s	$\nu_{14}(E')$	1328	1946 w	$\nu_{13} + \nu_{17}$ 1437 + 507 = 1944	
1338 w					
1343 w			1956 w	$^{10}B_3$	
1352 vw	$\nu_4 + \nu_{17}$ 845 + 507 = 1352		2055 w	$\nu_{14} + \nu_{18}$ 1326 + 734 = 2060	
			2230 vw	$\nu_8 + \nu_{14}$ 904 + 1326 = 2230	
1360 w					
1377 m 1379 m, sh 1381 m, sh 1387 sh 1399 w, br	Partially deuterated species		2240 vw		
			2290 w	$\nu_4 + \nu_{13}$ 845 + 1437 = 2282	
			2530 w		
1415 vw	$\nu_3 + \nu_{17}$ 904 + 507 = 1411		2560 vw		
			2850 vw		
1437 vs	$\nu_{13}(E')$	1440	2915 vw		
1440 sh	Partially deuterated species or $\nu_9 + \nu_{18}$ 713 + 734 = 1447		3457 m, sh 3462 m, sh	$\nu_3 + \nu_{12}$ 974 + 2529 = 3503	
			3480 s	$\nu_{11}(E')$	3485

[a] Gas data from ref 6.

modes, at 918 cm^{-1}. In the matrix this band has shifted to 910 cm^{-1}. The other A_2'' vibration was also undetected in the matrix, but a frequency of 380 cm^{-1} for the out-of-plane B–O–B ring bend, ν_7, was found in combination. This compares with 403 cm^{-1} for the similar B–N–B motion in borazine. The E′ assignments of Grimm, *et al.*, were confirmed. Using their predicted in-plane frequencies as a basis two of the A_1' modes, ν_2 and ν_3, were estimated at 906 and 800 cm^{-1}, respectively, and were observed in combination. Combination-mode fitting also allowed the two A_2' modes to be identified at 1477 and 1197 cm^{-1}, compared with the calculated frequencies of 1448 and 1183 cm^{-1}, respectively. The E″ modes, ν_{13} and ν_{14}, were observed in combination if vibrational frequencies of 1053 and 340 cm^{-1} were assumed, respectively. These compare with the observed frequencies of the isoelectronic molecule *s*-triazine, $H_3N_3C_3$, of 1031 and 340 cm^{-1}, respectively.[14]

The assigned frequencies of matrix-isolated boroxine, for the three isotopic species considered, are summarized in Table VIII. The product rule was applied where possible, and the results are presented in Table IX. The fit for the A_2' species is the poorest since the location of some of the shifted bands is in doubt (Table VIII).

(14) J. E. Lancaster, R. F. Stamm, and N. B. Colthup, *Spectrochim. Acta*, **17**, 155 (1961).

Discussion

It is interesting to note that in both borazine and boroxine the absorptions due to the B–H out-of-plane bend (913 and 910 cm^{-1}) and for borazine the N–H out-of-plane bend (718 cm^{-1}) as well have associated with them abnormal band structure. In borazine the bands at 718 and 913 cm^{-1} display a shoulder at lower frequencies and the relative intensity of the band due to the $^{10}B_3$-containing species is much stronger than is expected from the natural abundance of that species (Figure 1). In boroxine, there is a shoulder on ν_6 at a lower frequency, 905 cm^{-1}, and an unusually weak isotope structure at 921 and 929 cm^{-1} (Figure 4). The $\nu_6(A_2'')$ at 910 cm^{-1} shifts to 929 cm^{-1} in the case of 96% ^{10}B-enriched boroxine. The mixed isotopic species, with C_{2v} symmetry, transform the A_2'' species to B_1 and the E″ into $A_2 + B_1$. If these B_1 species overlap, Fermi resonance may shift one to lower and the other to higher

TABLE III

THE INFRARED SPECTRA OF $H_3B_3O_3$ AND $H_3{}^{10}B_3O_3$

$H_3{}^nB_3O_3$ in Ar matrix	Assignment	$H_3{}^nB_3O_3$ gas[a]	$H_3{}^{10}B_3O_3$ gas[a]	Assignment	$H_3{}^{10}B_3O_3$ in Ar matrix
530 m	$\nu_{12}(E')$	530			
534 w					
			537	$\nu_{12}(E')$	538 s
					730 vw
					775 vw
					820 vw, br
875 vw	$\nu_{12} + \nu_{14}$ 530 + 343 = 873				
				$\nu_{12} + \nu_{14}$ 538 + 347 = 885	885 vw
905 vw	$^{11}B_2{}^{10}B$				
910 s	$\nu_6(A_2'')$	918		$^{11}B_2{}^{10}B$	912 vw
920 vw	$^{11}B^{10}B_2$			$^{11}B^{10}B_2$	920 sh
930 w	$^{10}B_3$		935	$\nu_6(A_2'')$	929 s
974 m	B_2H_6 impurity				
				$^{10}B_2H_6$ impurity	978 w
985 vw	$\nu_{11}(E')$	990			
			1025	$\nu_{11}(E')$	1002 vw
1168 s	B_2H_6 impurity				
				B_2H_6 impurity	1172 vw
1180 vw	$\nu_3 + \nu_7$ 800 + 380 = 1180				
				$\nu_3 + \nu_7$ 802 + 388 = 1190	1190 vw
1208 m	$\nu_{10}(E')$	1213			
1215 w	$^{11}B_2{}^{10}B$			$^{10}B_2{}^{11}B$	1214 w
			1228	$\nu_{10}(E')$	1225 s
1330 m	$\nu_{12} + \nu_3$ 530 + 800 = 1330				
1333 w, sh	$\nu_{11} + \nu_{14}$ 990 + 343 = 1333				
				$\nu_{12} + \nu_3$ 538 + 802 = 1340	1340 m
1379 vs	$\nu_9(E')$	1389			
1381 sh					
1393 m	$\nu_{13} + \nu_{14}$ 1050 + 343 = 1393				
1404 vs	$^{11}B_2{}^{10}B$			$\nu_{13} + \nu_{14}$ 1060 + 347 = 1407	1398 m
1410 sh					1408 sh
1418 m	$^{11}B^{10}B_2$			$^{11}B^{10}B_2$	1418 sh
			1428	$\nu_9(E')$	1421 vs
					1432 sh
1435 vw	$\nu_{12} + \nu_2$ 530 + 906 = 1436				1442 sh
				$\nu_{12} + \nu_2$ 538 + 932 = 1470	1470 vw
1592 vs	B_2H_6 impurity				
				B_2H_6 impurity	1596 m
1825 w, br	$\nu_2 + \nu_6$ 906 + 910 = 1816				
				$\nu_2 + \nu_6$ 932 + 929 = 1861	1868 w
1882 w, br	$\nu_2 + \nu_{11}$ 906 + 990 = 1896				
				$\nu_2 + \nu_{11}$ 932 + 1002 = 1934	1892 vw
					2115 vw
					2125 vw
2160 w, br	BH_3CO impurity			BH_3CO impurity	2167 w, br
2335 vw, br	$\nu_9 + \nu_{11}$ 1379 + 990 = 2369				2410 vw, br
2460 m, br	BH_3CO impurity			BH_3CO impurity	2460 br
				$2\nu_8(?)$	2515 m
2524 vs	B_2H_6 impurity				
				B_2H_6 impurity	2530 w, sh

TABLE III (*Continued*)

$H_3{}^nB_3O_3$ in Ar matrix	Assignment	$H_3{}^nB_3O_3$ gas[a]	$H_3{}^{10}B_3O_3$ gas[a]	Assignment	$H_3{}^{10}B_3$ in Ar matrix
2576 m	$\nu_9 + \nu_5$ 1379 + 1197 = 2576				
2582 w	$^{11}B_2{}^{10}B$				2591 w
2592 m, sh	$\nu_9 + \nu_{10}$ 1379 + 1208 = 2587				2600 vw
2605 sh	B_2H_6 impurity				
2610 vs	$\nu_8(E')$	2620			
			2624	$\nu_8(E')$	2614 vs
2620 sh					
2630 sh					
				$\nu_9 + \nu_5$ 1421 + 1227 = 2648	2649 w
2768 w	$2\nu_9 = 2758$			or $\nu_9 + \nu_{10}$ 1421 + 1225 = 2646	
2850 w	$\nu_9 + \nu_4$ 1379 + 1477 = 2856				
2910 w	$\nu_8 + \nu_{14}$ 2610 + 343 = 2953				

[a] Gas phase data ref 9.

TABLE IV

THE INFRARED SPECTRUM OF $D_3B_3O_3$

$D_3{}^nB_3O_3$ in Ar matrix	Assignment	$D_3{}^nB_3O_3$ gas[a]	$D_3{}^nB_3O_3$ in Ar matrix	Assignment	$D_3{}^nB_3O_3$ gas[a]
522 m	$\nu_{12}(E')$	522	1325 s	$\nu_{12} + \nu_3$ 800 + 522 = 1322	
718 w	B_2D_6				
726 vw			1365 vs	$\nu_9(E')$	1373
			1374 sh	$\nu_{12} + \nu_{13}$ 522 + 852 = 1374	
748 w	$\nu_{11}(E')$	760			
758 w	$^{11}B_2{}^{10}B$		1381 s, sh	$\nu_2 + \nu_{12}$ 860 + 522 = 1382	
776 w			1391 vs	$^{11}B_2{}^{10}B$	
			1397 sh		
798 s, sh			1404 s	$^{11}B^{10}B_2$	
802 s	$\nu_6(A_2'')$	808			
810 ms	$^{11}B_2{}^{10}B$		1760 w	$\nu_5 + \nu_{11}$ 1012 + 748 = 1760	
814 m, sh					
			1770 vw	Isotopic species	
870 m	B_2D_6				
			1850 s	B_2D_6	
910 w					
			1885 vw	$\nu_9 + \nu_{12}$ 1365 + 522 = 1887	
1130 m	$\nu_{10}(E')$	1133			
1139 w	$^{11}B_2{}^{10}B$		1900 vw		
1145 vw	$^{11}B^{10}B_2$		1905 vw		
1155 vw	$\nu_3 + \nu_7$ 800 + 355 = 1155		1915 w		
			1937 s, sh	$\nu_3 + \nu_{10}$ 800 + 1130 = 1930	
1192 vs	B_2D_6				
			1948 vs	$\nu_8(E')$	1940
1225 vw	$\nu_2 + \nu_7$ 860 + 355 = 1215		1964 m, sh	$^{11}B_2{}^{10}B$	
			1980 s	B_2D_6	
			2160 vw, br	BH_3CO	
			2260 vw	$2\nu_{12} = 2(1130) = 2260$ or $\nu_8 + \nu_{14} = 1948 + 317 = 2265$	
			2340 vw, br	CO_2(?)	

[a] Gas phase data from ref 9.

TABLE V

RAMAN SPECTRUM OF $H_3B_3N_3H_3$

Gas phase	Matrix inferred	Assignment	Liquid[a]
270 wm[b]			
	280	$\nu_{20}(E'')$	288 wm, dp
290 wm[b]			
518 wm	518	$\nu_{17}(E')$	521 wm, dp
555 w		$2\nu_{20}(E' + A_1')$	
685 vw			
787 w	770	$\nu_{10}(E'')$	798 vw
857 vs, p	845	$\nu_4(A_1')$	852 s, p
892 w		$\nu_{17} + \nu_{10}(E'')$ 518 + 394 = 912	
942 vs, p	940	$\nu_3(A_1')$	940 vs, p
958 s, p		$^{11}B_2{}^{10}B$	953 sh, p
968 w, p		$^{11}B^{10}B_2$	968 w
976 vw, p		$^{10}B_3$	
987 w	977	$\nu_{18}(E'')$	968
1068 w, dp	1068	$\nu_{16}(E')$	1070 m, dp
		$\nu_{14}(E')$	1371 w, br, dp
		$\nu_{13}(E')$	1458 w, dp
2422 w			
2455 vw			
2505 vw, sh, dp		$\nu_{14} + \nu_{15}(E' + A_1')$ 1406 + 1096 = 2502	
2515 w, sh, dp	2513	$\nu_{12}(E')$	2510 w, sh, dp
2525 m, dp		$\nu_{13} + \nu_{16}(E' + A_1')$ 1465 + 1068 = 2533	
2545 vs, p		$\nu_2(A_1')$	2535 vs, p
2557 s, p		$^{11}B_2{}^{10}B$	
2570 w		$^{11}B^{10}B_2$	
2580 vw		$^{10}B_3$	
3473		$\nu_2 + \nu_3(A_1')$ 2545 + 942 = 3487	
3488 vs, p		$\nu_1(A_1')$	3453 vs, p
3490 w, sh		$\nu_{12} + \nu_{18}(E' + A_1')$ 2520 + 987 = 3507	
3523		$\nu_2 + \nu_{18}(E')$ 2535 + 987 = 3522	

[a] Liquid data from ref 6. [b] Center of band at 280 cm^{-1}.

TABLE VI

THE VIBRATIONAL FUNDAMENTALS OF BORAZINE[a]

		$H_3{}^{11}B_3N_3H_3$	$H_3{}^{10}B_3N_3H_3$	$D_3{}^{11}B_3N_3H_3$
A_1'	ν_1	(3488)[b]	(3488)	(3488)
	ν_2	(2545)	(2554)	(1893)
	ν_3	940	974	904
	ν_4	845	848	845
A_2'	ν_5	...	...	...
	ν_6	1195	1237	...
	ν_7	782	794	...
A_2''	ν_8	913	926	803
	ν_9	718	724	713
	ν_{10}	403	406	330
E'	ν_{11}	3482	3482	3480
	ν_{12}	2513	2529	1912
	ν_{13}	1458	1486	1437
	ν_{14}	1394	1404	1326
	ν_{15}	1102	1106	1020
	ν_{16}	1068	1072	812
	ν_{17}	518	528	507
E''	ν_{18}	977	985	734
	ν_{19}	770	770	760
	ν_{20}	280	285	260

[a] Frequencies observed in argon matrix. [b] Values in parentheses not observed but inserted from Raman data.

frequency. The effect in boroxine is very dramatic as the intensity of the bands is drastically reduced. Possible confirmation of the above argument is found in the

TABLE VII

PRODUCT RULE CALCULATIONS

Species	$H_3{}^{10}B_3N_3H_3/H_3{}^{11}B_3N_3H_3$ Theoret	$H_3{}^{10}B_3N_3H_3/H_3{}^{11}B_3N_3H_3$ Exptl	$D_3{}^{11}B_3N_3H_3/H_3{}^{11}B_3N_3H_3$ Theoret	$D_3{}^{11}B_3N_3H_3/H_3{}^{11}B_3N_3H_3$ Exptl
A_1'	1.049	1.048	0.707	...
A_2'	1.032	...	0.745	...
A_2''	1.029	1.030	0.720	0.715
E'	1.079	1.061	0.509	0.491
E''	1.032	1.026	0.745	0.689

TABLE VIII

VIBRATIONAL FUNDAMENTALS OF BOROXINE[a]

		$H_3{}^{11}B_3O_3$	$H_3{}^{10}B_3O_3$	$D_3{}^{11}B_3O_3$
A_1'	ν_1	(2616)[b]	(2630)	(1959)
	ν_2	906	932	860
	ν_3	(800)	802	800
A_2'	ν_4	1477	(1517)	(1470)
	ν_5	1197	(1227)	1012
A_2''	ν_6	910	929	808
	ν_7	(380)	388	(355)
E'	ν_8	2610	2614	1948
	ν_9	1379	1421	1365
	ν_{10}	1208	1225	1130
	ν_{11}	990	1002	748
	ν_{12}	530	538	522
E''	ν_{13}	1050	1060	852
	ν_{14}	343	347	(317)

[a] Frequencies observed in argon matrix. [b] Values in parentheses are estimated.

TABLE IX
PRODUCT RULE CALCULATIONS

Species	$H_3{}^{10}B_3O_3/H_3{}^{11}B_3O_3$ Theoret	$H_3{}^{10}B_3O_3/H_3{}^{11}B_3O_3$ Exptl	$D_3{}^{11}B_3O_3/H_3{}^{11}B_3O_3$ Theoret	$D_3{}^{11}B_3O_3/H_3{}^{11}B_3O_3$ Exptl
A_1'	1.049	1.037	0.707	0.711
A_2'	1.013	(1.053)	0.734	(0.841)
A_2''	1.030	1.042	0.720	(0.829)
E'	1.079	1.075	0.509	0.514
E''	1.013	1.020	0.734	0.749

absence of this structure in *B*-monosubstituted borazines.[15,16]

Fermi resonance is also invoked to understand the structure in the region from 1440 to 1490 cm^{-1} (Figure 2), already discussed to some extent before. The combination found for this region is $\nu_3 + \nu_{17}(E')$ at 1458 cm^{-1}. This combination shifts to 1502 cm^{-1} for ^{10}B-enriched samples. The symmetry of the combination is the same as for the fundamental. Hence Fermi resonance is allowed and both the combination band and the fundamental are shifted. Thus the gas-phase frequency of the fundamental is probably in error; in the matrix it is impossible to make a certain choice of the fundamental between the 1448- and the 1458-cm^{-1} bands and on the basis of intensity alone the 1458-cm^{-1} band was picked. The large amount of structure in the band system is due to the mixed-species combinations. Going from D_{3h} to C_{2v} for the $^{11}B_2{}^{10}B$ and $^{11}B^{10}B_2$ species, the A_1' is transformed into A_1, and the E', into $A_1 + B_1$. The combinations $A_1 \cdot A_1 = A_1$, and $A_1 \cdot B_1 = B_1$ are allowed, and hence there are four bands due to the two isotopic species. Similar arguments hold for the region from 2450 to 2700 cm^{-1}. In the case of 96% ^{10}B-enriched sample there are three bands in this region; presumably the other bands observed in the case of normal borazine are due to isotope structure. On this basis the 2513-cm^{-1} band is taken as the fundamental and the 2483- and 2522-cm^{-1} bands are assigned to $\nu_{14} + \nu_{15}(E')$ and $\nu_{13} + \nu_{16}(E')$, respectively. In combination the mixed species will produce four bands each, for a total of eight. This accounts for the rich structure. Much of this information is not available in the gas-phase infrared spectrum due to the rotational envelope. The complex structure near 1400 and 2600 cm^{-1} for boroxine is resolved in a manner similar to the one discussed above.

The assignments above were made with the assumption that both borazine and boroxine retain their gaseous structure in the matrix. While most bands have shifted from their gas-phase position by a few per cent, these shifts are much smaller than the shifts observed for molecules where strong interactions with the matrix occur. Experiments with mixed matrices prove that no strong matrix perturbations take place and rule out multiple trapping site effects. Degenerate modes are apparently not split. The observed complex structures discussed above can be understood in terms of the resonance interactions between strong fundamentals and combination bands occurring at nearly the same frequency. The selection rules in the matrix appear to follow those in the gas phase, leading to the conclusion that gaseous symmetry has been retained. These conclusions suggest further that of the two possible electron diffraction structures for borazine, the planar model is the more stable one and the only one present at low temperature.

The close correlation between the gaseous and liquid Raman spectra is surprising because it indicates that in liquid borazine there is very little association.

The borazine assignments reported here are in essential agreement with the calculated frequencies resulting from the recently published normal-mode treatment of Blick, Dawson, and Niedenzu,[17] although several of the actual frequencies used there need to be modified. It would appear that using their force constants as a starting point in a refinement would allow a very good force constant treatment of borazine. The inactive A_2' modes could certainly be calculated. By using the information available for borazine it was possible, through a combination-band analysis, to assign all the fundamentals of boroxine. The ring modes and those involving B–H modes compare for the two molecules remarkably well. It would now be possible to perform a normal-mode analysis for the out-of-plane modes of boroxine.

Acknowledgments.—We gratefully acknowledge financial support from the Army Research Office (Durham) and the Advanced Research Projects Agency (Materials Science Center, Cornell University).

(15) M. Oertel and R. F. Porter, *Inorg. Chem.*, **9**, 904 (1970).
(16) R. F. Porter and E. S. Yeung, *ibid.*, **7**, 1306 (1968).
(17) K. E. Blick, J. W. Dawson, and K. Niedenzu, *ibid.*, **9**, 1416 (1970).